Evaluation of Thermal Versus Plasma-Assisted ALD Al_2O_3 as Passivation for InAlN/AlN/GaN HEMTs

Anna Malmros, Piero Gamarra, Marie-Antoinette di Forte-Poisson, Hans Hjelmgren, *Senior Member, IEEE*, Cedric Lacam, Mattias Thorsell, *Member, IEEE*, Maurice Tordjman, Raphaël Aubry, and Niklas Rorsman, *Member, IEEE*

***Abstract*— Al_2O_3 films deposited by thermal and plasma-assisted atomic layer deposition (ALD) were evaluated as passivation layers for InAlN/AlN/GaN HEMTs. As a reference, a comparison was made with the more conventional plasma enhanced chemical vapor deposition deposited SiN_x passivation. The difference in sheet charge density, threshold voltage, f_T and f_{max} was moderate for the three samples. The gate leakage current differed by several orders of magnitude, in favor of Al_2O_3 passivation, regardless of the deposition method. Severe current slump was measured for the HEMT passivated by thermal ALD, whereas near-dispersion free operation was observed for the HEMT passivated by plasma-assisted ALD. This had a direct impact on the microwave output power. Large-signal measurements at 3 GHz revealed that HEMTs with Al_2O_3 passivation exhibited 77% higher output power using plasma-assisted ALD compared with thermal ALD.**

***Index Terms*— GaN HEMT, InAlN, passivation, ALD, Al_2O_3.**

I. Introduction

THE InAlN/AlN/GaN HEMT has recently gained increasing interest. In contrast to the conventional AlGaN/GaN heterostructure, InAlN may be grown lattice matched, which should be favorable from a reliability perspective. Furthermore, the built-in polarization field is higher in InAlN, enabling vertical and lateral downscaling, which promotes the high frequency performance [1], [2].

A problem with GaN HEMTs is electron trapping, which limits the microwave output power and linearity. The traps are located mainly at the semiconductor surface and in the GaN buffer layer. Deposition of a passivation layer mitigates the contribution from surface traps. On the negative side, passivation may result in undesired device characteristics, such as higher gate leakage and lower cutoff frequency.

Manuscript received January 13, 2015; revised January 16, 2015; accepted January 17, 2015. Date of publication January 22, 2015; date of current version February 20, 2015. This work was supported by the Swedish and French MoDs as part of the European Defence Agency project (MANGA), the Swedish Foundation for Strategic Research (SSF), and the Swedish Research Council (VR). The review of this letter was arranged by Editor T. Egawa.

A. Malmros, H. Hjelmgren, M. Thorsell, and N. Rorsman are with the Microwave Electronics Laboratory, Department of Microtechnology and Nanoscience, Chalmers University of Technology, Gothenburg 412 58, Sweden (e-mail: anna.malmros@chalmers.se).

P. Gamarra, M.-A. di Forte-Poisson, C. Lacam, and M. Tordjman are with the Epitaxial Growth of Wide Band-Gap Materials Laboratory, 3-5 Laboratory/Thales Research and Technology, Marcoussis 91460, France.

R. Aubry is with the GaN Process Laboratory, 3-5 Laboratory/Thales Research and Technology, Marcoussis 91460, France.

Color versions of one or more of the figures in this letter are available online at http://ieeexplore.ieee.org.

Digital Object Identifier 10.1109/LED.2015.2394455

The most common passivation for GaN HEMTs is SiN_x, deposited by Plasma Enhanced Chemical Vapor Deposition (PECVD) [2], [3]. In recent years, the use of Al_2O_3 deposited by Atomic Layer Deposition (ALD) has become more frequent [4], [5]. Two subcategories of ALD exist: thermal and plasma-assisted ALD. For thermal ALD water vapor is used as oxidant, while plasma-assisted ALD uses an oxygen plasma. Oxygen plasma is a very efficient oxidant, but any plasma treatment may cause ion-induced damage. In this letter Al_2O_3 deposited by thermal and plasma-assisted ALD were compared. They were used as passivation layers in InAlN/AlN/GaN HEMTs, which were characterized and evaluated in terms of DC, RF, pulsed IV, and large signal performance. Characterization of devices with the conventional PECVD SiN_x passivation was included for reference.

II. Fabrication

The heterostructure consisted of an AlN nucleation layer, a 1.6 μm thick GaN buffer layer, a 2 nm AlN interlayer, and a 6 nm $In_{0.19}Al_{0.81}N$ barrier layer, grown by MOCVD. The GaN buffer was non-intentionally doped. Instead the growth conditions were tuned in order to obtain semi-insulating properties. 2×50 μm HEMTs with a drain-source distance of 1.5 μm and 180 nm long centered gates were fabricated. Ta-based ohmic contacts were deposited and annealed at low temperature. More information on the growth and the processing can be found in [6]–[8]. The substrate was split into three pieces which were passivated individually. On the first piece, an Al_2O_3 film was deposited by thermal ALD at a rate of 0.85 Å/s. The second piece was also passivated with Al_2O_3, but by plasma-assisted ALD at a rate of 1.17 Å/s. In both cases the precursor was trimethyl aluminum (TMAl) and the chamber temperature 300 °C. The duration of the deposition was adjusted so that both films were 55 nm thick. The resulting refractive indices were similar: 1.63 (thermal ALD) and 1.64 (plasma-assisted ALD). The third piece was passivated with a 250 nm thick SiN_x layer, using a PECVD process at 340 °C. Finally, the three samples were annealed at a low-temperature (300 °C). The three device types are hereafter referred to as the thermal ALD HEMT, plasma-assisted ALD HEMT, and PECVD HEMT.

III. Results and Discussion

The main measurement results in this letter are listed in Table I. The Hall mobility was around 1550 cm^2/Vs for

TABLE I
SUMMARY OF MEASUREMENT RESULTS

Passivation/deposition method		Al_2O_3/ thermal ALD	Al_2O_3/ p.-a. ALD	SiN_x/ PECVD
n_s [cm^{-2}]		-1.53×10^{13}	-1.60×10^{13}	-1.66×10^{13}
μ [$cm^2V^{-1}s^{-1}$]		1575	1540	1555
R_{sheet} [$\Omega/\square$]		259	253	242
V_{th} [V], V_{ds} = 2 V		-1.1	-1.3	-1.5
g_m [mS/mm]		420	500	420
$I_{ds,max}$ [mA/mm][1]		775	876	923
DIBL, δV_{ds} = [14 15] V, [mV/V]		80	100	90
Slump ratio [%]	Z_1	-14.0	0.7	-3.1
	Z_2	-20.3	-2.1	-5.6
$P_{out,\,max}$ [W/mm]		1.9	3.3	2.4
η at P_{in} = 15 dBm [%]		56	40	52
$G_{T,max}$ [dB]		13	17	14
BV_{ds} [V]		29	21	19
BV_{dg} [V]		36	23	25

[1]Pulsed I_{ds} at (V_{gs}, V_{ds}) = (1, 3) V with a quiescent bias of (0, 0) V.

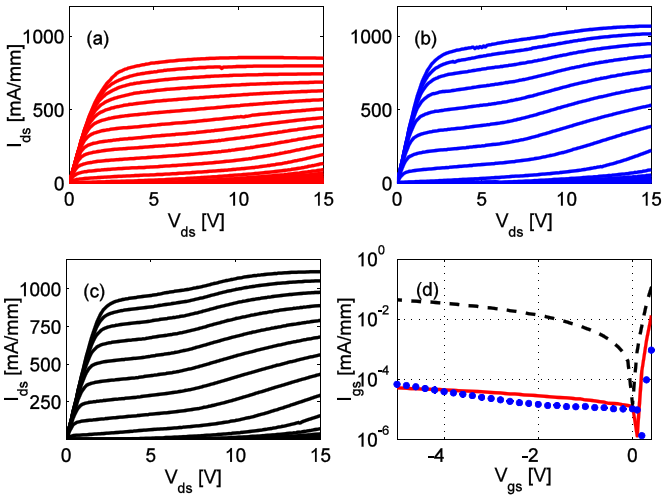

Fig. 1. DC output characteristics for HEMT with a) thermal ALD Al_2O_3, b) plasma-assisted ALD Al_2O_3, and c) PECVD SiN_x. d) Gate current vs gate voltage with grounded source and drain for thermal ALD Al_2O_3 (solid), plasma-assisted ALD Al_2O_3 (dots), and PECVD SiN_x (dashed).

all samples. Some variation was seen in the sheet electron density (n_s). The SiN_x passivated sample had an n_s of $-1.66\cdot10^{13}$ cm^{-2}. The Al_2O_3 samples exhibited 8 and 4% lower n_s, for thermal and plasma-assisted ALD, respectively. The variations in n_s resulted in different threshold voltages, a higher n_s leading to a more negative threshold voltage. DC characteristics are presented in Fig. 1 a-c. A transconductance (g_m) of 500 mS/mm was measured for the plasma-assisted ALD HEMT, while the other two exhibited a g_m of 420 mS/mm. The gate leakage current of the PECVD HEMT was several orders of magnitude higher than for the other two (Fig. 1d).

The Drain-Induced Barrier Lowering (DIBL) was calculated as a measure to estimate the short-channel effects, which were present in all three devices. DIBL was defined as $\delta V_{th}/\delta V_{ds}$, where δV_{ds} was the interval between 14 and 15 V. V_{th} was

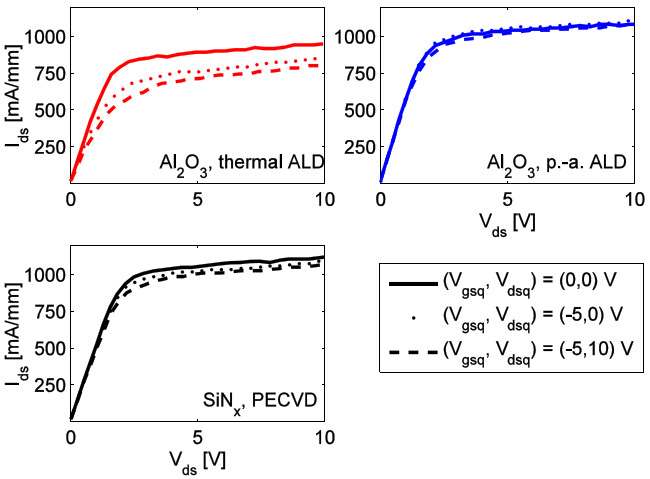

Fig. 2. Drain current pulsed from different quiescent bias points to $V_{gs} = +1$V.

obtained by extrapolation from the inflection point of the I_{ds} curve. Although the thermal ALD HEMT appeared to have a smaller DC output conductance, only minor differences were seen in the DIBL (Table I).

S-parameters measured up to 110 GHz showed that the RF performance of the three devices was comparable, exhibiting an f_{max} of 90–100 GHz and f_T of 39–47 GHz.

Pulsed IV measurements were performed to investigate lag effects (Fig. 2). The drain and gate voltages were pulsed from a quiescent bias point (V_{gsq}, V_{dsq}) to a final voltage of +1 V on the gate, and 0–10 V on the drain. The pulse length was 0.5 μs and the the pulse separation time was 1 ms. The slump ratio was defined as

$$Z_n = \frac{I_{ds,Vdsq,Vgsq} - I_{ds,0,0}}{I_{ds,0,0}}. \quad (1)$$

Two slump ratios, Z_1 and Z_2, corresponding to (V_{gsq}, V_{dsq}) = $(-5, 0)$ V and $(-5, 10)$ V, respectively, were calculated. The mean values for all drain biases are presented in Table I. The deposition method had a large impact on the current slump. Severe current slump was seen for the thermal ALD HEMT, while hardly any dispersion could be measured for the plasma-assisted ALD HEMT. Little, but not insignificant current slump was seen for the PECVD HEMT.

The absence of current slump in one device indicates that the slump effects were dominated by surface traps. Notably, no correlation between the gate leakage and gate lag was found, as opposed to what has been suggested elsewhere [9], [10].

Load-pull measurements were performed at 3 GHz (Fig. 3), with the setup described in [11]. The drain bias was set to 15 V and the load impedances were optimized for maximum output power. The output power correlated directly to the current slump. This resulted in an output power density of 3.3 W/mm of the plasma-assisted ALD HEMT, compared to 1.9 W/mm for the thermal ALD HEMT. The PECVD HEMT exhibited an output power density of 2.4 W/mm. The moderate performance of this device was associated partly with dispersion, and partly with a higher gate leakage, causing a voltage drop across the barrier layer. The maximum transducer gain ($G_{T,max}$) varied

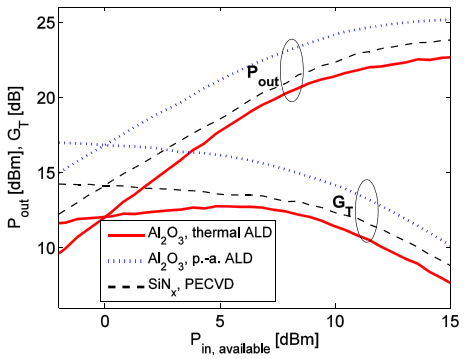

Fig. 3. Output power and transducer gain at 3 GHz for V_{ds} = 15V. The devices were biased for class AB operation.

from 13 to 17 dB, and the associated drain efficiencies from 40 to 56% (Table I).

The two- and three-terminal off-state breakdown voltages were measured as described in [12]. Notably, the thermal ALD HEMT exhibited by far the highest BV_{ds} (29 V). This was attributed to filled surface traps, depleting the channel and thereby causing a larger voltage drop between the drain terminal and the channel under the gate. Hence, a higher drain voltage was required to achieve the same voltage drop over the barrier. This passivation also resulted in the highest BV_{dg} (Table I). The PECVD HEMT had the lowest BV_{ds} (19 V), which was attributed to the higher gate leakage. For this device the gate current increased more rapidly with gate voltage, requiring less drain voltage to maintain the set drain current.

IV. Conclusion

This letter elucidated the impact of Al_2O_3 deposition by thermal and plasma-assisted ALD on the InAlN/AlN/GaN HEMT performance. Very low gate leakage currents were observed for both passivation methods, as opposed to the HEMT with the conventional PECVD SiN_x passivation. Plasma-assisted ALD resulted in near-dispersion free HEMTs, which translated into an output power of 3.3 W/mm. Thermal ALD, on the other hand, resulted in quite significant current slump, leading to a reduced output power (1.9 W/mm). The off-state breakdown voltage was, however, considerably higher for the thermal ALD HEMT.

References

[1] P. Saunier *et al.*, "InAlN barrier scaled devices for very high f_T and for low-voltage RF applications," *IEEE Trans. Electron Devices*, vol. 60, no. 10, pp. 3099–3104, Oct. 2013.

[2] S. Tirelli *et al.*, "Fully passivated AlInN/GaN HEMTs with f_T/f_{MAX} of 205/220 GHz," *IEEE Electron Device Lett.*, vol. 32, no. 10, pp. 1364–1366, Oct. 2011.

[3] A. Crespo *et al.*, "High-power Ka-band performance of AlInN/GaN HEMT with 9.8-nm-thin barrier," *IEEE Electron Device Lett.*, vol. 31, no. 1, pp. 2–4, Jan. 2010.

[4] D. Xu *et al.*, "0.2-μm AlGaN/GaN high electron-mobility transistors with atomic layer deposition Al_2O_3 passivation," *IEEE Electron Device Lett.*, vol. 34, no. 6, pp. 744–746, Jun. 2013.

[5] H. Wang *et al.*, "Al_2O_3 passivated InAlN/GaN HEMTs on SiC substrate with record current density and transconductance," *Phys. Status Solidi C*, vol. 7, no. 10, pp. 2440–2444, Oct. 2010.

[6] M.-A. di Forte Poisson *et al.*, "LP MOCVD growth of InAlN/GaN HEMT heterostructure: Comparison of sapphire, bulk SiC and composite SiCopSiC substrates for HEMT device applications," *Phys. Status Solidi C*, vol. 7, no. 5, pp. 1317–1324, May 2010.

[7] A. Malmros, H. Blanck, and N. Rorsman, "Electrical properties, microstructure, and thermal stability of Ta-based ohmic contacts annealed at low temperature for GaN HEMTs," *Semicond. Sci. Technol.*, vol. 26, no. 7, p. 075006, Jul. 2011.

[8] A. Malmros *et al.*, "Evaluation of an InAlN/AlN/GaN HEMT with Ta-based ohmic contacts and PECVD SiN passivation," *Phys. Status Solidi C*, vol. 11, nos. 3–4, pp. 924–927, Apr. 2014.

[9] W. S. Tan *et al.*, "Surface leakage currents in SiN_x passivated AlGaN/GaN HFETs," *Electron Device Lett.*, vol. 27, no. 1, pp. 1–3, Jan. 2006.

[10] N. Ramanan, B. Lee, and V. Misra, "Device modeling for understanding AlGaN/GaN HEMT gate-lag," *IEEE Trans. Electron Devices*, vol. 61, no. 6, pp. 2012–2018, Jun. 2014.

[11] M. Thorsell and K. Andersson, "Fast multiharmonic active load–pull system with waveform measurement capabilities," *IEEE Trans. Microw. Theory Techn.*, vol. 60, no. 1, pp. 149–157, Jan. 2012.

[12] S. R. Bahl and J. A. del Alamo, "A new drain-current injection technique for the measurement of off-state breakdown voltage in FETs," *IEEE Trans. Electron Devices*, vol. 40, no. 8, pp. 1558–1560, Aug. 1993.